

RADIATIVE FEEDBACK AND THE PHOTOEVAPORATION OF INTERGALACTIC CLOUDS

PAUL R. SHAPIRO^{1,2}, ALEJANDRO C. RAGA², GARRELT MELLEMA²

¹*Department of Astronomy, University of Texas, Austin, TX 78712, USA*

²*Instituto de Astronomía-UNAM, Apdo Postal 70-264, 04510 México D. F., México*

³*Stockholm Observatory, S-133 36 Saltsjöbaden, Sweden*

ABSTRACT. The first sources of ionizing radiation to condense out of the dark and neutral IGM sent ionization fronts sweeping outward through their surroundings, overtaking other primordial gas-clouds and photoevaporating them. Results are presented of the first gas dynamical simulations of this process, including radiative transfer, along with some observational diagnostics.

1. Ionization Fronts in the IGM

The rôle of hydrogen molecules as cooling agents in primordial gas clouds, necessary to form the first stars out of a gas of H and He with no heavier elements, is intimately related to the fate of those clouds in the presence of ionizing and dissociating radiation. That such radiation had an important effect on these primordial clouds is certain. The neutral, opaque IGM out of which the first bound objects condensed was dramatically reheated and reionized at some time between a redshift $z \approx 50$ and $z \approx 5$ by the radiation released by some of these objects (cf. [1] and references therein). When the first sources turned on, they ionized their surroundings by propagating weak, R-type ionization fronts which moved outward supersonically with respect to both the neutral gas ahead of and the ionized gas behind the front, racing ahead of the hydrodynamical response of the IGM [2,3]. The effect of density inhomogeneity on the rate of I-front propagation was previously described by a mean “clumping factor” $c_I > 1$, which slowed the I-fronts by increasing the average recombination rate per H atom inside clumps. This suffices to describe the rate of I-front propagation as long as the clumps are either not self-shielding or, if so, only absorb a fraction of the ionizing photons emitted by the central source. What is the dynamical effect of the I-front on the density inhomogeneity it encounters, however?

The answer depends on the size and density of the clumps overtaken by the I-front. The fate of linear density fluctuations depends upon their Jeans number, $L_J \equiv \lambda/\lambda_J$, the wavelength in units of the baryon Jeans length in the IGM at temperatures of order 10^4K . Fluctuations with $L_J < 1$ find their growth halted and reversed (cf. [4]). For nonlinear density fluctuations, however, the answer is more complicated, depending upon at least three dimensionless parameters, their internal Jeans number, $L_J \equiv R_c/\lambda_J$, the ratio of the cloud radius R_c to the Jeans length λ_J inside the cloud at about

10⁴K, their “Strömgen number” $L_s \equiv R_c/\ell_s$, the ratio of the cloud radius R_c to the Strömgen length ℓ_s inside the cloud (the length of a column of gas within which the unshielded arrival rate of ionizing photons just balances the total recombination rate), and their optical depth to H ionizing photons at 13.6 eV, τ_H , before ionization. If $\tau_H < 1$, the I-front sweeps across the cloud, leaving an ionized gas at higher pressure than its surroundings, and exits before any mass motion occurs in response, causing the cloud to blow apart. If $\tau_H > 1$ and $L_s > 1$, however, the cloud shields itself against ionizing photons, trapping the I-front which enters the cloud, causing it to decelerate inside the cloud to the sound speed of the ionized gas before it can exit the other side, thereby transforming itself into a weak, D-type front preceded by a shock. Typically, the side facing the source expels a supersonic wind backwards towards the source, which shocks the IGM outside the cloud, while the remaining neutral cloud material is accelerated away from the source by the so-called “rocket effect” as the cloud photoevaporates (cf. [5]). As long as $L_J < 1$ (the case for gas bound to dark halos with virial velocity less than 10 km s⁻¹), this photoevaporation proceeds unimpeded by gravity. For halos with higher virial velocity, however, $L_J > 1$, and gravity competes with pressure forces. For a uniform gas of H density $n_{H,c}$, located a distance r_{Mpc} (in Mpc) from a UV source emitting $N_{\text{ph},56}$ ionizing photons (in units of 10⁵⁶s⁻¹), the Strömgen length is only $\ell_s \cong (50 \text{ pc})(N_{\text{ph},56}/r_{\text{Mpc}}^2)(n_{H,c}/0.1 \text{ cm}^{-3})^{-2}$. We focus in what follows on the self-shielded case which traps the I-front. Some of these results were summarized previously by us in [6].

2. The Photoevaporation of an Intergalactic Cloud Overtaken by a Cosmological Ionization Front

As a first study of these important effects, we have simulated the photoevaporation of a uniform, spherical, neutral, intergalactic cloud of gas mass $1.5 \times 10^6 M_\odot$, radius $R_c = 0.5 \text{ kpc}$, density $n_{H,c} = 0.1 \text{ cm}^{-3}$ and $T = 100 \text{ K}$, in which self-gravity is unimportant, located 1 Mpc from a quasar with emission spectrum $F_\nu \propto \nu^{-1.8}$ ($\nu > \nu_H$) and $N_{\text{ph}} = 10^{56} \text{ s}^{-1}$, initially in pressure balance with an ambient IGM of density 0.001 cm^{-3} which at time $t = 0$ has just been photoionized by the passage of the intergalactic R-type I-front generated when the quasar turned on. [A standard top-hat perturbation which collapses and virializes at $z_{\text{coll}} = 9$, for example, with total mass $\cong 10^7 M_\odot$, has circular velocity $v_c \cong 7 \text{ km s}^{-1}$, $R_c \cong 560 \text{ pc}$, and $n_{H,c} = 0.1 \text{ cm}^{-3}$, if $\Omega_b h^2 = 0.03$ and $h = 0.5$.] Apart from H and He, the cloud also contains heavy elements at 10⁻³ times the solar abundance. Our simulations in 2D, axisymmetry use an Eulerian hydro code (called CORAL), with Adaptive Mesh Refinement and a Riemann solver based on the Van Leer flux-splitting algorithm, which solves nonequilibrium ionization rate equations (for H, He, C, N, O, Ne, and S) and includes an explicit treatment of radiative transfer by taking into account the bound-free opacity of H and He [7,8,9]. Our grid size in cylindrical coordinates (r, x) was 128×512 cells (fully refined).

Most current simulations of cosmological gas dynamics which include photoionization do so by approximating the radiation field as uniform and isotropic, ignoring the inhomogeneity of the radiation field and setting optical depth to zero. To illustrate the importance of a more realistic approach to radiative transfer, we present results for two

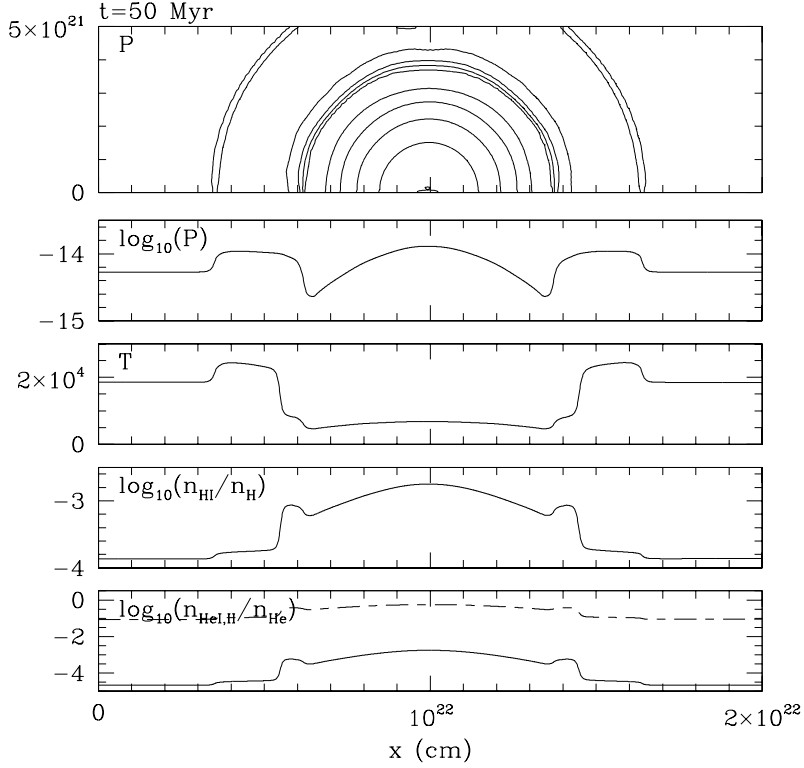


Fig. 1. ZERO OPTICAL DEPTH APPROXIMATION. One time-slice 50 Myr after turn-on of quasar located 1 Mpc away from cloud to the left of computational box along the x -axis. From top to bottom: (a) isocontours of pressure, logarithmically spaced, in (r, x) -plane of cylindrical coordinates; (b) pressure along the $r = 0$ symmetry axis; (c) temperature; (d) H I fraction; (e) He I (solid) and He II (dashed) fractions.

cases in what follows: (1) zero optical depth and (2) optical depth properly included. Figure 1 shows the structure of the cloud 50 Myr after it was overtaken by the quasar’s I-front as it sweeps past the cloud in the IGM when optical depth is neglected. The cloud and IGM are both instantaneously photoionized everywhere in this case, causing the overpressured cloud to expand isotropically into the surrounding IGM, acting as a spherical piston which sweeps up the IGM and drives a shock into it. The cloud matter eventually expands as a shell and evacuates a spherical hole. The column densities of H I, He I and II, and C IV for cloud gas of different velocities as seen along the symmetry axis at different times are shown in Figure 3. This cloud would initially resemble a velocity-broadened Lyman alpha forest quasar absorber (“LF”) 10’s of km s^{-1} wide, with $N_{\text{HI}} > 10^{16} \text{cm}^{-2}$, which evolves toward a narrower LF absorber with $N_{\text{H,I}} < 10^{15} \text{cm}^{-2}$,

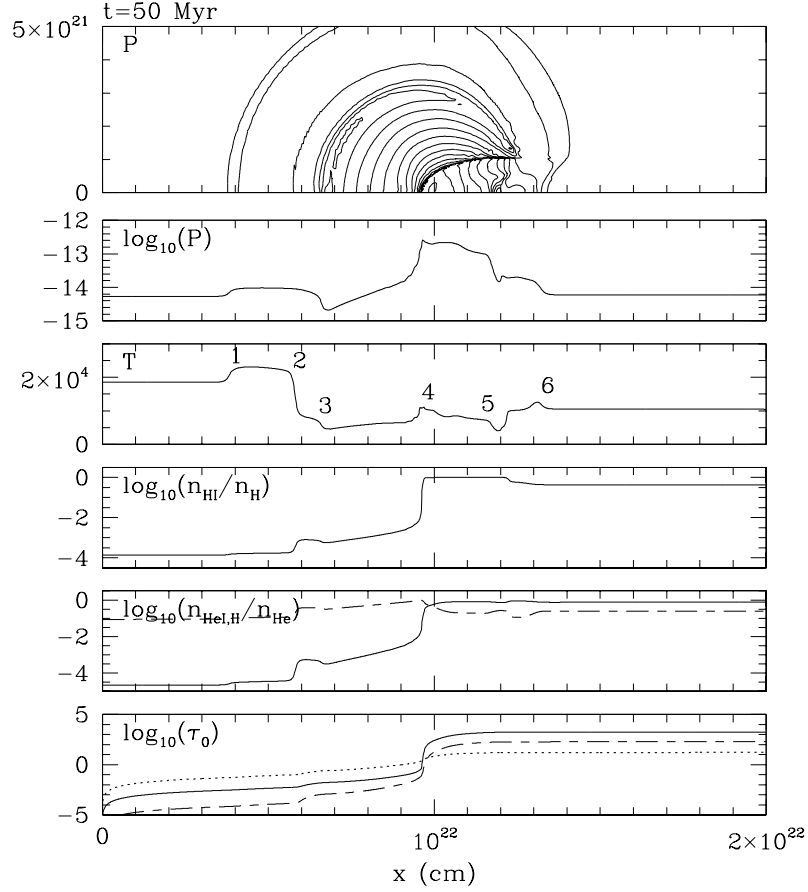


Fig. 2. Same as Figure 1, except: OPTICAL DEPTH INCLUDED. Bottom panel is bound-free optical depth along $r = 0$ axis at the threshold ionization energies for H I (solid), He I (dashed), He II (dotted).

with $N_{\text{HeII}}/N_{\text{HI}} \leq 10^2$ and $N_{\text{CIV}} \sim 10^{12} \text{cm}^{-2}$ throughout. As the spatial variations for the relative abundances of selected metal ions at 50 Myr plotted in Figure 5 show, only highly ionized metals are present in this case. By contrast, we show results for all these same quantities from the simulation which takes proper account of optical depth, instead, in Figures 2, 4, and 6. Since $\ell_S \ll R_c$ initially, the cloud traps the I-front, as described above, and drives a supersonic wind from the surface facing the quasar. It takes more than 100 Myr to evaporate the cloud, accelerating it to 10's of km s^{-1} in the process. Key features of the flow are indicated by the numbers which label them on the temperature plot in Figure 2: 1 = IGM shock; 2 = contact discontinuity between shocked cloud wind and swept up IGM; 3 = wind shock; between 3 and 4 = supersonic wind; 4 = I-front; 5 = shock preceding I-front; 6 = shock that leads the motion of remain-

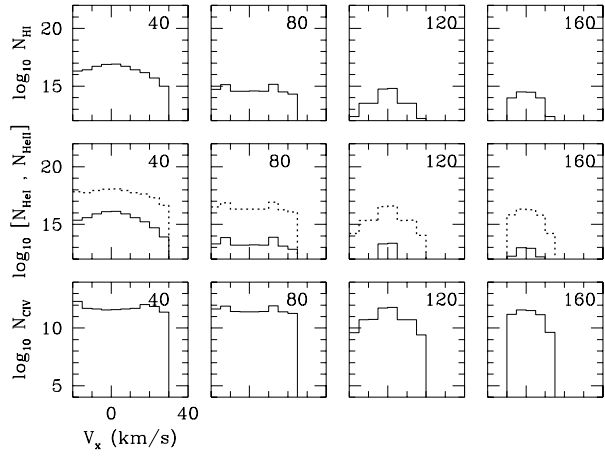


Fig. 3. Cloud column densities (cm^{-2}) along symmetry axis at different velocities: ZERO OPTICAL DEPTH APPROXIMATION. From top to bottom: (top) H I; (middle) He I (solid) and He II (dotted); (bottom) C IV. Each box labelled with time (in Myrs) since QSO turn-on.

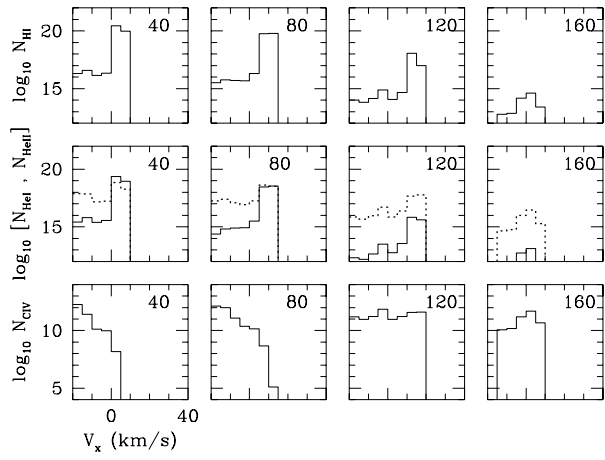


Fig. 4. Same as Figure 3, except OPTICAL DEPTH INCLUDED.

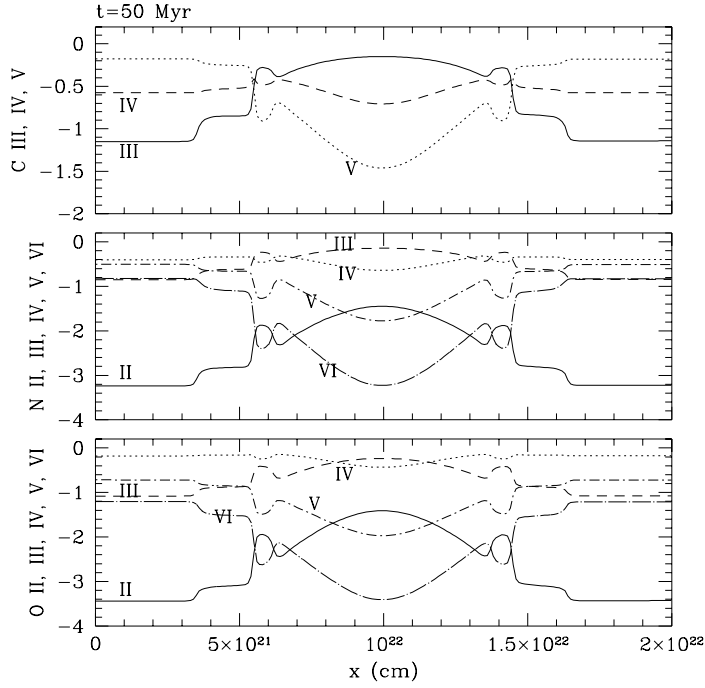


Fig. 5. Carbon, Nitrogen, and Oxygen Ionic Fractions Along Symmetry Axis at $t = 50$ Myr: ZERO OPTICAL DEPTH APPROXIMATION.

ing neutral cloud gas into the shadow region. At early times, the cloud gas resembles a weak Damped Lyman Alpha (“DLA”) absorber with small velocity width ($\sim 10 \text{ km s}^{-1}$) and $N_{\text{HI}} \sim 10^{20} \text{ cm}^{-2}$, with velocity-broadened LF-like wings (width $\sim 20 \text{ km s}^{-1}$) with $N_{\text{HI}} \sim 10^{16} \text{ cm}^{-2}$ on the side moving toward the quasar, with a C IV feature with $N_{\text{CIV}} \sim 10^{12} \text{ cm}^{-2}$ displaced in this same asymmetric way from the velocity of peak H I column density. After 160 Myr, however, only a narrow H I feature with LF-like column density $N_{\text{HI}} \sim 10^{14} \text{ cm}^{-2}$ remains, with $N_{\text{HeII}}/N_{\text{HI}} \sim 10^2$ and $N_{\text{CIV}}/N_{\text{HI}} \sim [\text{C}]/[\text{C}]_{\odot}$. Unlike the zero-optical-depth approximation, Figure 6 shows the presence at 50 Myrs of low as well as high ionization stages of the metals.

Acknowledgements

This work was supported by NASA Grant NAG5-2785 and NSF Grant ASC-9504046, and was made possible by a UT Dean’s Fellowship and a National Chair of Excellence, UNAM, Mexico awarded by CONaCYT in 1997 for PRS.

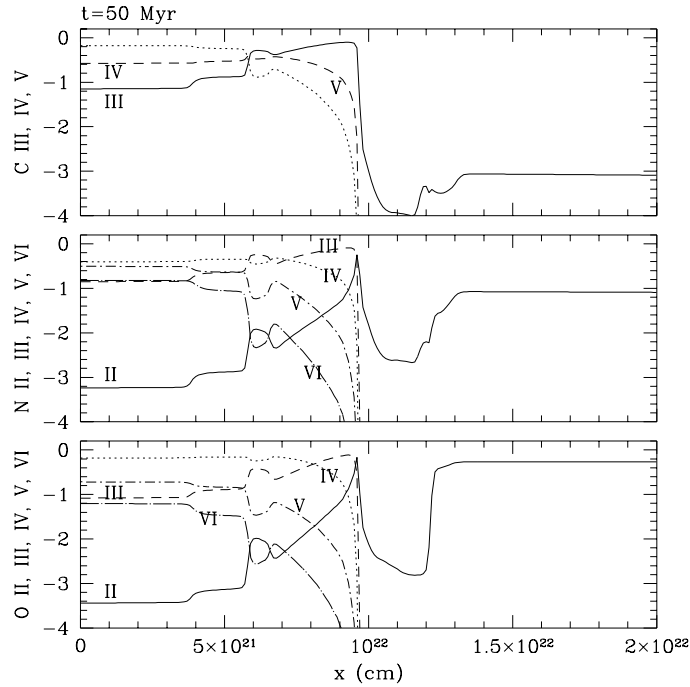


Fig. 6. Same as Figure 5, except OPTICAL DEPTH INCLUDED.

References

- [1] Shapiro, P. R. 1995, in *The Physics of the Interstellar Medium and Intergalactic Medium*, A. Ferrara, C. F. McKee, C. Heiles, and P. R. Shapiro eds., ASP Conf. Vol. 80, 55–97.
- [2] Shapiro, P. R. 1986, *Publ. Astr. Soc. Pacific* **98**, 1014
- [3] Shapiro, P. R., & Giroux, M. L. 1987, *Astrophys. J. Lett.* **321**, L107.
- [4] Shapiro, P. R., Giroux, M. L., & Babul, A. 1994, *Astrophys. J.* **427**, 25.
- [5] Spitzer, L. 1978, *Physical Processes in the Interstellar Medium* (Wiley).
- [6] Shapiro, P. R., Raga, A. C., & Mellema, G. 1997, in *Structure and Evolution of the Intergalactic Medium From QSO Absorption Line Systems*, P. Petitjean and S. Charlot eds., Editions Frontières, pp. 41–45.
- [7] Mellema, G., Raga, A. C., Canto, J., Lundqvist, P., Balick, B., Steffen, W., & Noriega-Crespo, A. 1997, *Astron. Astrophys.*, submitted.
- [8] Raga, A. C., Taylor, S. D., Cabrit, S., & Biro, S. 1995, *Astron. Astrophys.* **296**, 833.
- [9] Raga, A. C., Mellema, G., & Lundquist, P. 1997, *Astrophys. J. Suppl.* **109**, 517.